Bull. Mater. Sci., Vol. 25, No. 3, June 2002, pp. 219–225. © Indian Academy of Sciences.

Microstructure characterization of fluidized bed nitrided Fe–Si and Fe–Si–Al foils

H ATMANI* and O THOUMIRE

Groupe de Physique des Matériaux – UMR 6634 CNRS, UFR des Sciences, Université de Rouen – Evreux, BP 281, 27002 Evreux, France

MS received 20 August 2001; revised 26 March 2002

Abstract. This work deals with the structural modifications of FeSi and FeSiAl foils when subjected to a thermochemical nitriding treatment (TNT) performed in a fluidized-bed laboratory furnace. The investigations on the nitrided samples were carried out by optical and SEM microscopic observations, X-ray diffraction and Mössbauer spectroscopy. Both the compound and diffusion layers were investigated.

Keywords. Fe–Si; Fe–Si–Al foils; thermochemical nitriding treatment; fluidized-bed; structure; nitriding mechanism.

1. Introduction

Fe–Si foils are well known for their good soft magnetic properties and consequently have wide industrial applicability. Many studies have been carried out in the past to improve the properties of such systems and large amount of literature is available on the material structure and its connection with physical or technical properties (Brissoneau 1980; Arai and Ishiyam 1988; Krivastava and Vishwamittar 1988; Dabrowski and Zgodzinski 1989; Boc *et al* 1990; Shimizu *et al* 1990; Hayakawa and Szpunar 1997).

Commonly, industrial FeSi foils receive a thin layer (2–5 μm thick) of insulating mineral coating (for example, Mg_2SiO_4). This coating, which sticks perfectly with the surface of the material, produces mechanical constraints on the subjacent matrix. This leads to improvement of magnetic properties of the material.

Thermochemical nitriding treatment (TNT) is a suitable surface treatment process which enhances the hardness, wear and corrosion resistance of steels. The diffusion of nitrogen atoms and chemical surface modifications produce structural modifications leading to substantial improvements in the properties of the material (Billard *et al* 1990; Kooi *et al* 1994; Boettger *et al* 1997; Niederdrenk *et al* 1996; Schaaf 1998). The compound layer resulting from the nitriding treatment meets some of the criteria for electrical insulating and matrices under constraint which improve mechanical properties. Strict control of the modifications of the properties resulting from such a treatment could lead to the material being used for some particular applications.

In this paper, we briefly describe the experimental procedure of fluidized-bed thermochemical nitriding treatment (TNT). Then, we present the structural properties obtained with FeSi and FeSiAl foils when subjected to such treatments, especially the observed depth of the nitrided area and the nitrogen diffusion mechanism resulting from various parameters of the nitriding treatment. We have revealed the nitrided (i.e. compound + diffusion) layer. The analysis of the compound layer with the identification of the phases created at each depth stage enables such a layer to be described.

2. Experimental

The Fe (96·8 wt%) Si (3·2 wt%) and Fe (97·55 wt%) Si (2 wt%) Al (0·45 wt%) foils were industrially available. The samples were mechanically prepolished with a series of sandpapers (1200 grit) and with polishing cloths (3 μm). The samples were about 300 μm thick; the grain size was up to 1 mm for Fe–Si and 270 μm for Fe–Si–Al.

The nitriding of the samples were performed in a laboratory fluidized-bed furnace (Iacob and Vigier 1992; Iacob *et al* 1994). The fluidized sand composed of alumina particles. The gas used was ammonia (NH_3). The dissociation rate depended on the temperature; at a temperature equal to or higher than 500°C, the ammonia dissociated following the reaction:

$$NH_3 \rightarrow N + \tfrac{3}{2} H_2.$$

The dissociation of ammonia (ratio of 90%) allowed the atomic nitrogen to penetrate into the sample. The parameters contributing to TNT are temperature, time, gas flow and alumina particle size. The samples were treated following the conditions indicated in table 1. The

*Author for correspondence

alumina particle size was chosen to be constant and equal to 200 μm.

The nitrogen distribution in the sample was carried out by electronic microprobe analysis (EDAX 9100 Philips) performed on a cross section. The microstructure was examined both by optical microscopy and scanning electron microscopy (either by JEOL JSM 35 CF or JEOL 6100 equipped with a NORAN EDS analyser). The investigations of the new phases formed after different treatments were carried out by X-ray diffraction (XRD) with an INEL 120 CPS device using the Co-Kα radiation (l = 0·17909 nm) as well as by Mössbauer spectrometry. Because the sample was quite thick and TNT is a surface treatment, we used the conversion electron mössbauer spectrometry (CEMS) technique. The measurements were carried out at room temperature.

3. Results and discussion

3.1 *TNT (560–8–04) FeSi sample*

3.1a *Microscopic observations and XRD analysis*: The microstructure of TNT (560–8–04) (see table 1 for details) FeSi sample revealed by optical microscopy is shown in figure 1. Two distinct domains were observed. The outermost domain near the surface, was the nitrided layer with a constant thickness over the periphery of the sample.

Table 1. The experimental parameters of the thermochemical nitriding treatment (NTT).

	Temperature (°C)	Time (h)	Gas flow (m^3N/h)
TNT (560–8–04)	560	8	0·4
TNT (700–8–04)	700	8	0·4
TNT (560–8–0·7)	560	8	0·7

It extended towards the grain boundaries. The second domain represented the core of the sample. The nitrided layer consisted of a compound layer followed by a diffusion layer. The compound layer made its way between and on the grain boundaries following an inter- and intragranular diffusion of nitrogen. In figure 1, the continuity of the compound layer towards a large grain boundary was observed over the whole thickness, thus linking the two sides of the sample. The SEM investigations (figure 2) confirmed this phenomenon and showed even better the structure and the precipitates in the diffusion layer. The outermost region of about 6 μm depth showed the best penetration of nitrogen. Then, the nitrogen diffused giving rise to needle-like structure. The large needle precipitates could reach 100 μm in length, thus connecting the "compound-layer" with the inside of the matrix. Small needle precipitates of about 2 μm in size were also observed in the diffusion layer and in the core of the sample. Iron nitrides were formed within the needle-like precipitates: probably $Fe_4N(g')$ in large needles and $Fe_{16}N_2(a'')$ in small needles; however, the a''-phase was not detected by other techniques. The precipitation of such a phase has been revealed in FeN martensite (Van Genderen *et al* 1997).

The microstructure observed by optical and scanning electron microscopy on a cross-section of the TNT (560–8–04) Fe–Si–Al sample is reported in figures 3 and 4, respectively: the compound layer and the needle-like precipitates have been revealed. For either FeSi or FeSiAl, nitrogen diffuses both inter- and intragranularly. This is explained by the higher grain size measured for the samples and implying thus a few grain boundaries.

The EDS investigations, carried out on a cross-section of the sample, confirm the presence of nitrogen in the compound layer. Moreover, it seems to be that silicon and aluminium would migrate in the core of the sample.

The peaks of the XRD spectrum (figure 5) could be mainly indexed as the $Fe_4N(g')$ and $Fe_{2-3}N(e)$ nitrides.

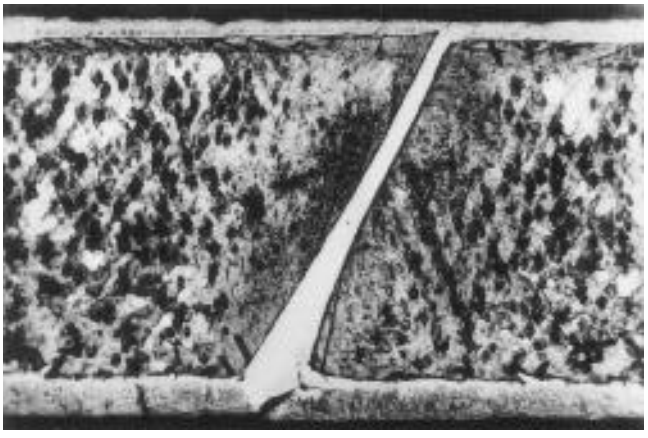

Figure 1. Optical photograph showing the microstructure of a nitrided FeSi sample at 560°C, 8 h, 0·4 m^3N/h. Nitrogen diffuses towards a grain boundary.

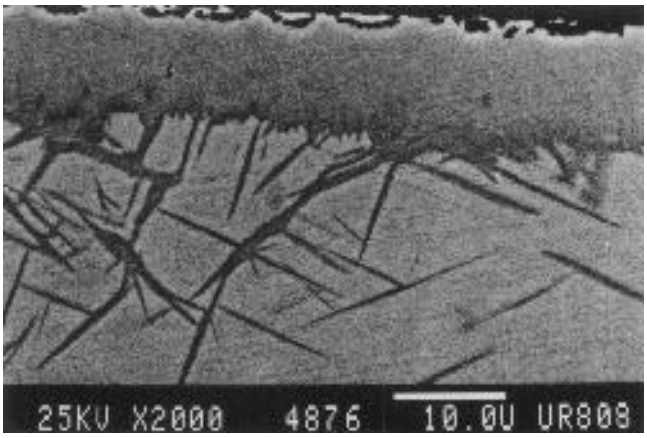

Figure 2. SEM photograph obtained with a nitrided FeSi sample at 560°C, 8 h, 0·4 m^3N/h.

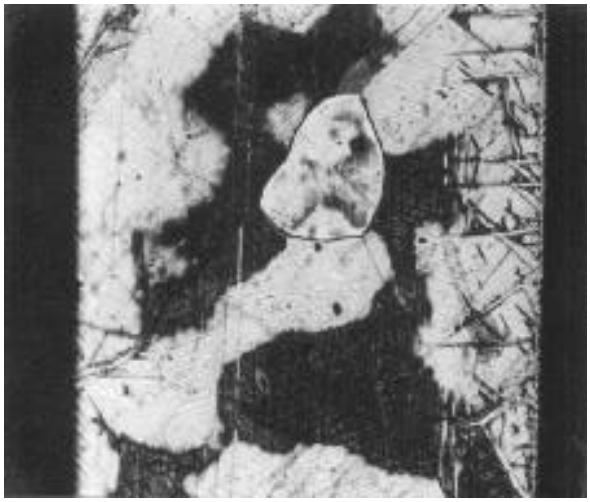

Figure 3. Optical photograph obtained with FeSiAl sample nitrided at 560°C, 8 h, 0·4 m^3N/h.

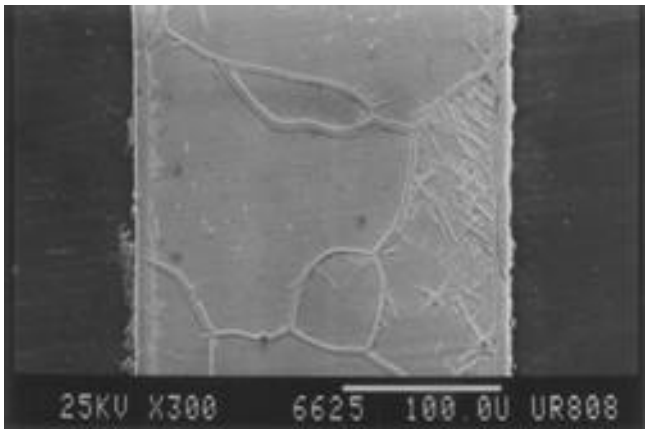

Figure 4. SEM photograph obtained with a nitrided FeSiAl sample at 560°C, 8 h, 0·4 m^3N/h.

Such nitrides were the main phases in the compound layer. The presence of Al and Si nitrides is not to be completely excluded. However, the techniques used did not allow such nitrides to be identified. Such precipitates, because of their small size together with their slight quantities would be "swamped" in the iron nitrides. The *a*-Fe phase was also identified and the peaks with weak intensities were indexed as Fe_2O_3 and Fe_3O_4 oxides. Such oxides with slight contents would be due to oxygen or moisture present in ammonia gas or formed on the surface suddenly after their exit from the furnace. In fact, some samples were not progressively cooled in the nitrogen atmosphere inside the bed, but removed from the furnace immediately after nitriding process.

The same is true for the FeSiAl sample. In the following, we focus our discussion on the FeSi sample.

3.1b *Mössbauer analysis*: After nitriding treatment, and by progressive polishings, we eliminated three thin superficial layers and systematically obtained a Mössbauer spectrum after each polishing operation. This allowed each phase present at each depth of the nitrided area to be identified. Thus, the compound layer could be reconstituted. The spectra obtained after different operations (figure 6) are labelled 2, 3 and 4. Spectrum 1, taken immediately after nitriding treatment, was fitted with Fe_2O_3, Fe_3O_4, *g*-Fe, $Fe_{2-3}N$ and Fe_4N phase contributions. Spectrum 2 was fitted with the Fe_3O_4, $Fe_{2-3}N$ and Fe_4N phase contributions; the austenite and Fe_2O_3 phases disappeared after first prepolishing. Spectrum 3 was fitted with the same contributions as spectrum 2, but with lower Fe_3O_4 oxide content. In the last spectrum (4), the oxide phase as well as the $Fe_{2-3}N$ phase completely disappeared. These phases existed in the surface layer up to a depth of 3 μm, in agreement with the microscopic observations. Spectrum 4 was therefore, fitted with Fe_4N, *a*-Fe and FeSi phase contributions; the bulk of the sample was reached. This suggests the hypothesis

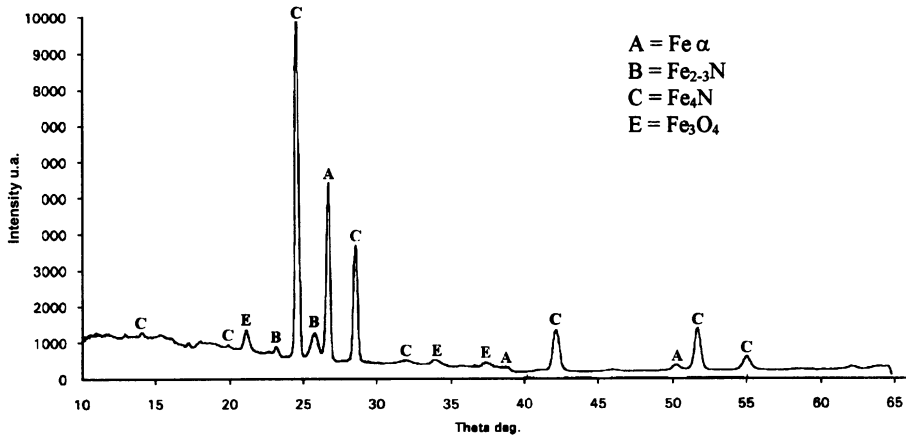

Figure 5. XRD spectrum of nitrided FeSi sample (560°C, 8 h, 0·4 m^3N/h).

Table 2. The concentration of the phases determined from the Mössbauer measurements for each spectrum. It concerns a layer of 0·1 μm depth.

	g–Fe–N?	Fe_3O_4	$Fe_{2-3}N$	Fe_4N	*a*-Fe	*a*-Fe + Si
Spectrum 1	13%	49%	22%	16%	–	–
Spectrum 2	–	45%	39%	16%	–	–
Spectrum 3	–	26%	34%	40%	–	–
Spectrum 4	–	25%	–	–	54%	21%

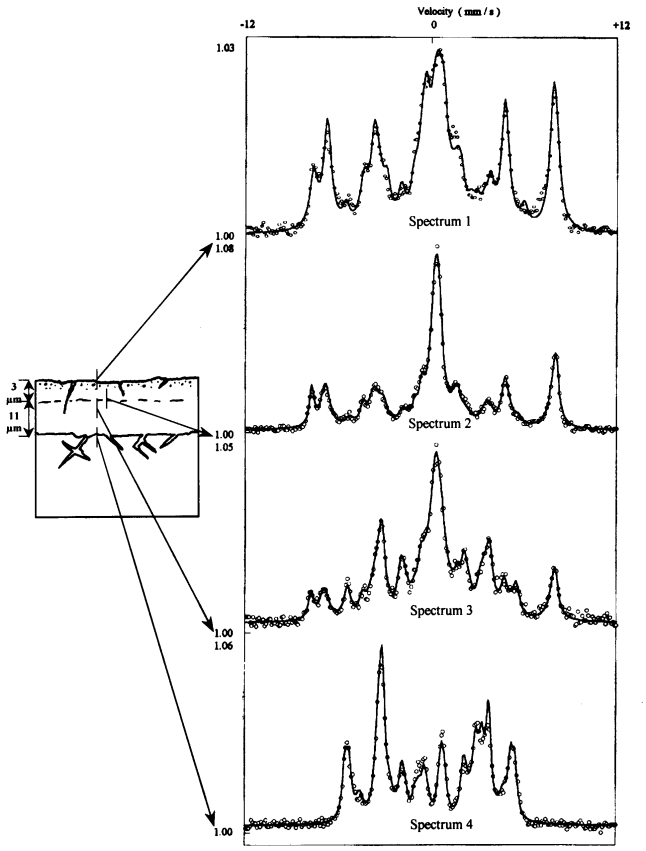

Figure 6. Mössbauer spectra of nitrided FeSi sample after successive prepolishings.

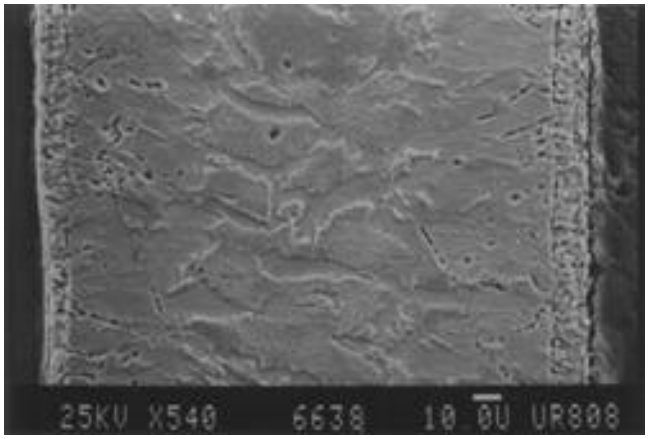

Figure 7. SEM photograph obtained with the FeSi sample nitrided with a gas flow of 0·7 m^3N/h.

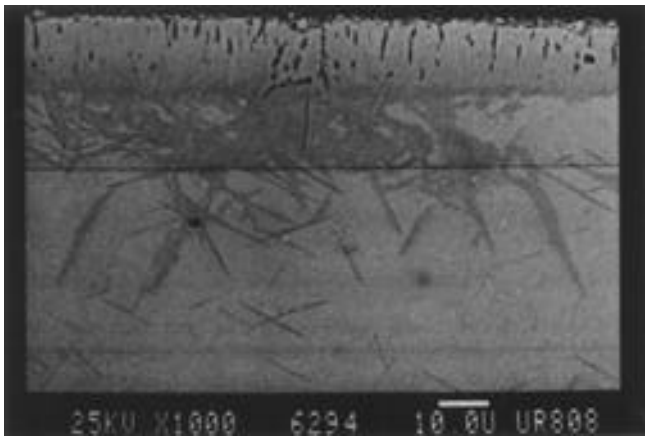

Figure 8. SEM photograph obtained with FeSiAl sample nitrided at 700°C; a porous-like microstructure is observed. The same is true for the FeSi sample.

according to which silicon is driven towards the core of the sample. However this remains to be explained. The concentrations of the phases are reported in table 2. It has to be noted that the concentrations obtained from the Mössbauer measurements only concern a layer of 0·1 μm depth.

3.2 *TNT (560–8–07) FeSi sample*

The compound layer of the sample was affected by the treatment performed with a gas flow equal to 0·7 m^3N/h. The microstructure clearly showed a porous-like aspect (figure 7). The pores near the surface played the role of diffusion channels between the surface and inside of the sample. These channels enable the same conditions of treatment either for the outer surface or for the inside of the compound layer to be satisfied. The formation of this layer is, therefore, extended to a limit depth where the gas regeneration is stopped. This phenomenon has already been observed in other systems (Somers and Mittemeijer 1990). The XRD analysis shows no significant differences as compared with the TNT (560–8–04). The same phases are detected. The peak intensity of the $Fe_{2-3}N$ phase was less. This could be explained by the decreasing content of such a phase.

3.3 *TNT (700–8–04) FeSi sample*

The microstructure revealed by SEM with a FeSi sample nitrided at 700°C is shown in figure 8. The limit between the compound layer and the diffusion zone is not clearly distinguishable. The microphotograph shows a porous-like structure. The pores could be explained by the diffusion channels following the process described in subsection 3·2. At this temperature, the penetration depth of the nitrogen is not far below the surface because of the rapid recombination.

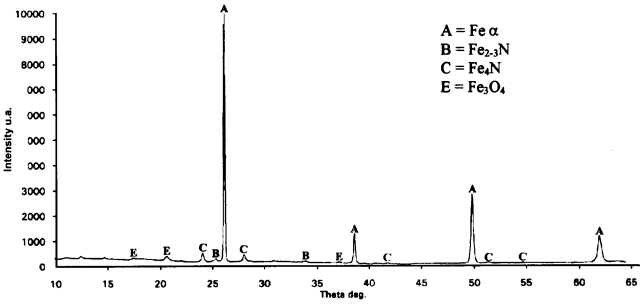

Figure 9. XRD spectrum of nitrided FeSi (700°C, 8 h, $Q = 0{\cdot}4$ m^3N/h).

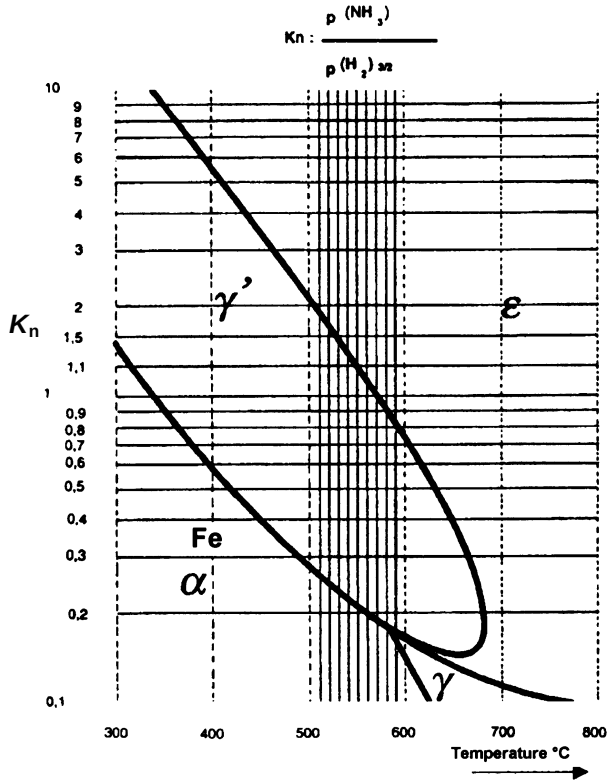

Figure 10. Lehrer diagram showing different phases vs the K_n parameter and the temperature.

The corresponding XRD peaks (figure 9) have been mainly indexed by the α-Fe phase. The peaks with low intensities are indexed with $Fe_{2-3}N$ and Fe_4N nitrides. The Fe_2O_3 and Fe_3O_4 oxides have also been identified. The Mössbauer spectrum obtained with the same sample is fitted with the Fe_2O_3 and Fe_3O_4 contributions as well as with that of the α-Fe phase; the corresponding concentrations were 27%, 21% and 52%, respectively. To identify the phases underneath the oxide-layer, we have eliminated the surface layer by successive prepolishings as we did for NTT (560–8–04) treatment. After the last prepolishing, the Fe_3O_4 oxide still existed but in low concentration. This was probably due to the prepolishing method which cannot be precisely controlled and so does not completely eliminate the surface layer. No nitrides, or silicon were detected immediately underneath the oxide layer. The absence of the iron nitrides underneath the oxide layer may be explained by the diagram of Lehrer (figure 10) (Lehrer 1930). In the diagram are shown the different phases versus the temperature and versus K_n ($K_n = p(NH_3)/p(H_2)^{3/2}$) coefficient. For $T = 700$°C, the partial pressures, $p(NH_3)$ and $p(H_2)$ corresponding to the dissociation of the ammonia ($NH_3 \rightarrow N + 3/2\ H_2$) are $3{\cdot}1 \times 10^{-5}$ and $7{\cdot}5 \times 10^{-1}$ respectively. This allows K_n to be determined. Thus, for $T = 700$°C and $K_n = 4{\cdot}8 \times 10^{-5}$, only the solid solution γ-Fe is expected to be formed. The formation of α-Fe phase in our case, can be explained by the extrapolation of the α-domain limit $\leftrightarrow$ γ-domain limit towards the small values of K_n. While, at temperature of 560°C, the K_n coefficient is higher than 0·2. Following the diagram, this allowed the Fe_4N and $Fe_{2-3}N$ nitrides to be formed.

3.4 *Nitriding mechanism*

The nitriding treatment of the FeSi and FeSiAl foils

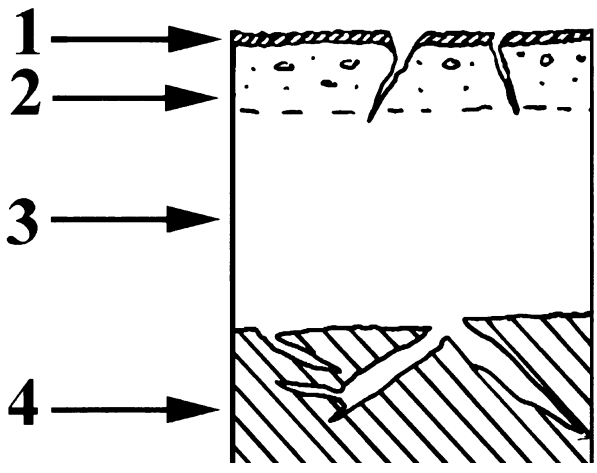

Figure 11. Illustration of the nitrided sample showing different area: 1 = very thin layer (not exactly identified), 2 = $Fe_{2-3}N + Fe_3O_4$ layer, 3 = Fe_4N layer and 4 = diffusion layer.

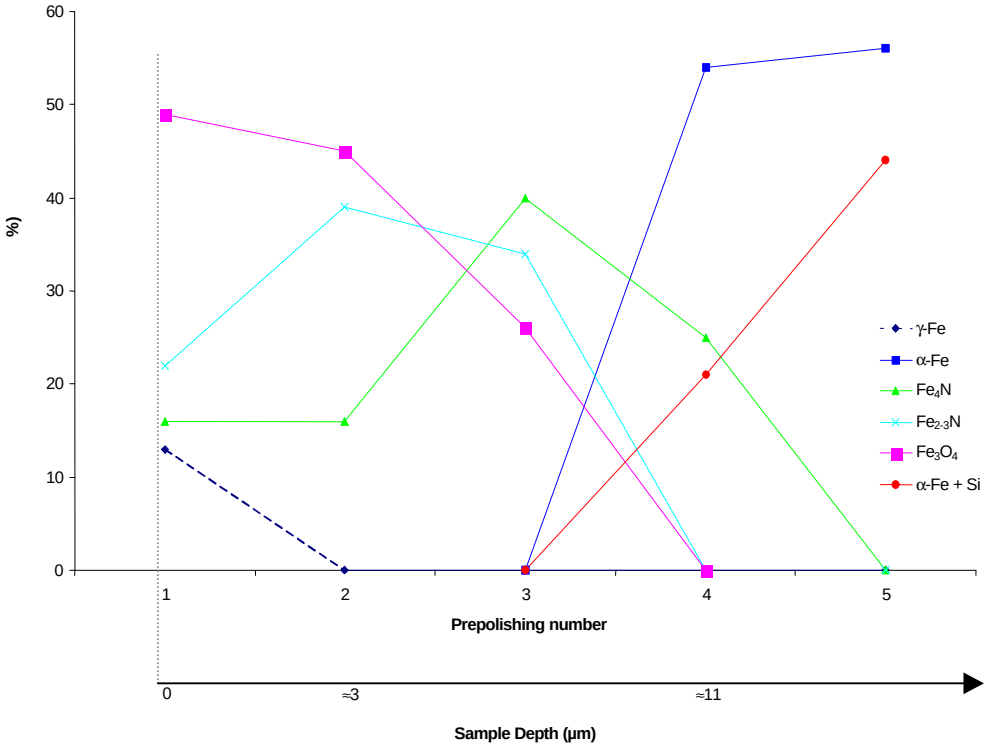

Figure 12. Phase content evolution vs the penetration depth according to results of table.

allows the compound layer and the diffusion layer to be revealed. Starting from the surface and going towards the core of the sample, the following phases in relation with the penetration depth have been identified: (i) "very thin layer", not exactly identified, (ii) layer of both $Fe_{2-3}N$ (*e*) nitride and Fe_3O_4 oxide, (iii) layer of Fe_4N (*g′*) nitride and diffusion layer.

It has to be noted that the very thin layer in the outermost surface has been adjusted by a paramagnetic phase (it could be indexed by the (*g*–Fe–(N)?) by means of the Mössbauer technique. However, such a phase has not been confirmed by X-ray diffraction; its content could be very weak (in a zone of 0·1 µm thick) to be detectable. The hypothesis of an artefact or an unknown phase is not either excluded. Moreover, the diffusion area has been observed with an impoverishment of silicon and aluminium.

The nitriding mechanism is illustrated in figure 11. The variation of the concentration of the different phases in relation with the nitriding depth is shown in figure 12.

4. Conclusions

Thermochemical nitriding treatment has been used as a surface treatment for FeSi and FeSiAl foils. The compound layer depth is estimated to be about 10 µm followed by the diffusion layer. The compound layer is diphasic with two nitride-types: $Fe_{2-3}N$ and Fe_4N. In the diffusion layer, the Fe_4N and the *a*-Fe phases have been identified. Both for FeSi and FeSiAl samples, a needle-like structure is observed. The nitrided layer is poor in silicon and aluminium. This remains to be explained. A porous-like structure is observed when the sample is treated either with a temperature of 700°C or with gas flow equal to 0·7 m^3N/h. The pores play the role of channels linking the outer atmosphere and the inside of the compound layer allowing thus a better penetration of nitrogen. It is worth noting that TNT is considered as a surface treatment, and consequently the results concern particularly the nitrided layer.

References

Arai K I and Ishiyam K 1988 *J. Appl. Phys.* **64** 5352
Billard A, Foos M, Frantz C and Gantois M 1990 *Surf. Coatings Tech.* **43–44** 521
Boc I, Cziraki A, Csebi J, Nemeth S and Szentmiklosi L 1990 *IEEE Trans. Magn.* **26** 2226
Boettger A, Genderen M L, Han K and Mittemeijer E J 1997 *J. Phys. IV* **17(C5)** 257
Brissoneau P 1980 *J. Magn. Magn. Mater.* **19** 52
Dabrowski M and Zgodzinski J 1989 *J. Phys. Scr.* **40** 40
Hayakawa Y and Szpunar J A 1997 *Acta Mater.* **45** 1285

Iacob C and Vigier P 1992 *Traitement de surface en lit fluidisé* (Paris: PYC) p. 97

Iacob C, Vigier P, Thoumire O, Vu Dinh J, Malandin J J and Labulle B 1994 *Traitement Thermique* **270** 33

Kooi B J, Somers M A J and Mittemeijer E I 1994 *Metall. Mater. Trans.* **A25** 2797

Krivastava S and Vishwamittar J 1988 *J. Magn. Magn. Mater.* **74** 316

Lehrer E 1930 *Z. Electrochem.* **36** 383

Niederdrenk M, Schaaf P, Lieb K P and Schulte O 1996 *J. Alloys and Compounds* **237** 81

Schaaf P 1998 *Hyperfine Inter.* **111** 113

Shimizu R, Harase J and Dingley D J 1990 *Acta Mater.* **38** 973

Somers M A and Mittemeijer E J 1990 *Metall. Trans. A, Phys. Metall. Mater. Sci.* **A21** 189

Van Genderen M J, Bottger A and Mittemeijer E J 1997 *Metall. Mater. Trans. A, Phys. Metall. Mater. Sci.* **28** 63